Study of Plasmon-Exciton Interactions in Metal-Semiconductor Nanoparticles

A thesis submitted towards partial fulfilment of the BS-MS Dual Degree Program

by

ABHIJIT FULKAR

under the guidance of

PROF. SULABHA K. KULKARNI

and

DR. G. V. PAVAN KUMAR

Indian Institute of Science Education and Research (IISER), Pune

Certificate

This is to certify that this dissertation entitled "*Study of Plasmon-Exciton Interactions in Metal-Semiconductor Nanoparticles*" submitted towards partial fulfilment of the BS-MS dual degree programme at Indian Institute of Science Education and Research, Pune represents work carried out by **Abhijit Fulkar** at Indian Institute of Science Education and Research, Pune under the supervision of **Prof. Sulabha K. Kulkarni** and **Dr. G. V. Pavan Kumar**, Department of Physics during the academic year 2016-2017.

Abhijit Fulkar

Reg. no: 20121056

Dr. G. V. Pavan Kumar

Assistant Professor

Committee:

Prof. Sulabha K. Kulkarni (supervisor)
Dr. G. V. Pavan Kumar (co-supervisor)
Dr. C. V. Dharmadhikari (TAC)

Declaration

I hereby declare that the matter embodied in the report entitled "*Study of Plasmon-Exciton Interactions in Metal-Semiconductor Nanoparticles*" are the results of thework carried out by me at the Department of Physics, Indian Institute of Science Education and Research, Pune, under the supervision of **Prof. Sulabha K. Kulkarni** and **Dr. G. V. Pavan Kumar** and the same has not been submitted elsewhere for any other degree.

Abhijit Fulkar

Reg. no: 20121056

Dr. G. V. Pavan Kumar

Assistant Professor

Dedicated to my family

Acknowledgements

I would like to express my gratitude to my dissertation advisor, Professor Sulabha Kulkarni, for motivating me and mentoring me for the last four years. Her guidance moulded me into the researcher that I am today. I would also like to thank Dr. Smita Chaturvedi, for all the help and advice she has given over the course of my research.

I'm very grateful to Professor G.V. Pavan Kumar, for agreeing to be my supervisor when Professor Sulabha had to take a leave due to certain unfortunate circumstances.

I want to thank my lab mates Harjot and Kavya for all the intellectual thesis related discussions. I'm also grateful to my friends Varun, Omkar, Shalini, Irene and Vished for helping me in different aspects. I would also like to thank Amey, Prashant and Priyank for their never-ending support throughout the project.

And lastly, I would like to thank IISER Pune and all other people who have supported me directly or indirectly in the completion of this project.

Abstract

We studied the properties of gold and CdTe/CdSe nanostructures using different characterization techniques. Coupling of plasmons in metal nanoparticles with exciton in semiconductor nanoparticles shows fascinating optical properties. Due to the interaction between a di-electric confined electronic state in metals and quantum confined electronic states in semiconductors shows clampdown of emission profile in gold nanospheres, gold nanorods with CdTe QDs. Also, we have done some preliminary study with CdSe QDs with gold nanospheres. Hence, the coupling of plasmon-exciton interaction leads to control of the energy-transfer process. Also, we can tune the emission and absorption profiles which can have probable applications in light emitting diodes, photovoltaic systems, sensors, etc.

Contents

Table of Figures

Chapter 1: Introduction

Metal nanostructures have been a subject of intensive research for their fascinating surface plasmon resonance (SPR) properties while semiconductor nanostructures because of their size dependent properties and applications in different fields. Both of the materials at nano-scale sizes display fascinating properties.

Size dependent optical tuning in entire visible electromagnetic spectrum enables one to understand the quantum confinement effect in semiconductor nanostructures while dielectric confinement in metal nanostructures. At this scale, intriguing properties such as optical, electrical and magnetic were observed. Due such properties these materials have potential applications such as light emitting diodes, photovoltaic systems, etc.

1.1 LSPR in metal nanoparticles

In 1857, M. Faraday recognized the existence of metal nanoparticles in solution and a quantitative explanation of their colour was given by G. Mie in 1908. This metal nanoparticle solution was of gold which shows red intense colour.[1][2]

G. Mie explained the colour by finding solution to Maxwell's equations where he considered interaction of light with uniform spherical gold particles dispersed in dielectric medium.

He observed decrease in intensity, when electromagnetic radiation is incident on the uniform spherical particles in a medium.

When a beam of electromagnetic radiation having intensity I_0 with wavelength λ passes through a medium with dielectric constant ε_m. It was assumed that particles are uniform throughout the medium and the applied electromagnetic field also remains the same with every spherical particle. This is assumed so that the multiple reflections between these particles should not take place. Then the Beer-Lambert's law can be stated in the terms of transmitted intensity as,

$$I = I_0 e^{-\mu x}$$

where, 'μ' is the extinction co-efficient and 'x' is the length of the dielectric system where particles are well-dispersed, the schematic illustration of such system is shown in the figure below:

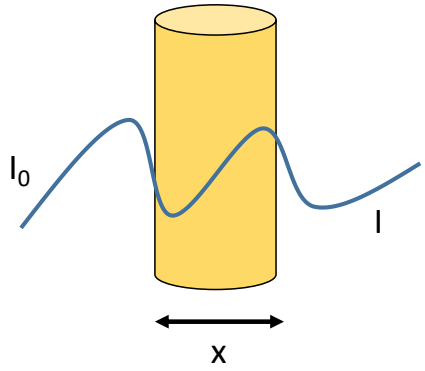

Figure 1: *Illustration of EM radiation with intensity I_o passing through medium with transmitted intensity I*

Here, extinction co-efficient is

$$\mu = \frac{N}{V C_{ext}}$$

C_{ext} is the extinction cross-section of the particle, N is the number of particles in the medium and V is the volume of the colloidal particles. C_{ext} is defined as,

$C_{ext} = C_{abs} + C_{sca}$

From Mie theory, extinction, absorption and scattering cross-sections were calculated which are as follows.

$$C_{ext} = \frac{2\pi}{k^2} \sum_{l=1}^{\infty} (2l+1)\, R_e\, (a_l + b_l)$$

Where a_l and b_l are co-efficient of scattering. These co-efficient are functions of a and λ in terms of Ricatti-Bessel functions and k is defined as

$$k = \frac{2\pi\sqrt{\varepsilon_m}}{\lambda}$$

For very small particles having radius R (kR ≪1), the extinction cross section is primarily because of the absorption. Hence, the extinction co-efficient can be given as

$$C_{ext} = \frac{24\pi^2 R^3 \varepsilon_m^{3/2}}{\lambda} \frac{\varepsilon_2}{(\varepsilon_2 + 2\varepsilon_2)^2 + \varepsilon_2{}^2}$$

$$\varepsilon(\omega) = \varepsilon_1(\omega) + i\varepsilon_2(\omega)$$

here,

$\varepsilon(\omega)$ is the dielectric constant of the particle. $\varepsilon_1(\omega)$ and $\varepsilon_2(\omega)$ are real and imaginary parts of the dielectric constant.

From the above equation, it is seen that C_{ext} directly depends on R^3. We know that, absorption co-efficient μ is inversely proportional to 1/V (=1/R^3). Hence absorption is the particle size independent. Also from the same equation, extinction cross-section will have maxima when

$$\varepsilon_1 + 2\varepsilon_m = 0$$

or

$$\varepsilon_1 = -2\varepsilon_m \text{ (if } \varepsilon_2 \text{ is small)}$$

This in turn results into strong resonance band. The peak height and bandwidth is calculated by $\varepsilon_2(\omega)$ (it is due to disappearance of C_{ext} if $\varepsilon_2 = 0$ or $\varepsilon_2 = \infty$).

In 1912, R. Gans modified the Mie theory to deal with ellipsoidal particles. According to Gans theory, the absorption of the particle depends only on the aspect ratio of the particle. In our work, we are dealing with gold nanospheres as well as gold nanorods, this theory will be useful. Hence to calculate absorption profile for ellipsoidal particles, shape factor or polarization is related to the three-dimension of the particle.

Using Mie's theory, one can calculate the absorption profile of nanoparticles of approximately 20 nm in size. One caveat however, is that the red-shifts in the absorption spectra are unexplained by Mie's theory as the dipole approximation does not suffice in this situation and careful speculation requires the consideration of both the particle size and the dielectric constant. The Drude model for metals provides an accurate description of the dielectric response in the free electrons of the metal. The localized surface plasmon resonance (LSPR) in the free electrons of metals is thus modelled using the Drude model.

Given, Drude model, Consider, the term plasma is defined as the free electrons in the conduction band. When light is irradiated on a metal surface, the loosely bound free electrons oscillates about their fixed ions with the frequency of light. Such quantized collective oscillations are termed as plasmons and its corresponding frequency called plasma frequency is defined as

$$\omega_p = \sqrt{\frac{ne^2}{m\varepsilon_o}}$$

where, m is the mass of electron, ε_o is the permittivity of free space, e is the charge of electron and n is the conduction electron density.

The phenomenon called surface plasmon resonance occurs when an electromagnetic radiation with frequency equal to frequency of the surface electrons incident on the metal surface. So, in simple terms, it is the coherent oscillation of the surface electrons.

In smaller size (less than 200 nm) nanoparticles, localized surface plasmon resonance is observed. In LSPR, the surface electrons collectively oscillate with the incident photons. They display enhanced near-field amplitude at the resonance wavelength.

When plasma frequency of a metal is equal to the frequency of the incident photo, surface plasmon resonance arises.

Consider a free conduction electron model and consider dielectric function as a combination of an interband term $\varepsilon_{IB}(\omega)$ and Drude term $\varepsilon_D(\omega)$ which can be stated as

$$\varepsilon(\omega) = \varepsilon_{IB}(\omega) + \varepsilon_D(\omega)$$

Here, $\varepsilon_D(\omega)$ is defined by the expression given below.

$$\varepsilon_D(\omega) = 1 - \frac{\omega_p^2}{\omega^2 + i\gamma\omega}$$

where ω_p is the plasma frequency in bulk metal defined in equation above. Damping constant is denoted by γ which is equal to the plasmon absorption bandwidth (In the limit $\gamma \ll \omega$ for a perfectly free electron gas).

The damping constant can be defined as follows which is related to lifetimes of electron scattering processes (electron-photon, electron-electron, electron-defect) in a bulk material[3].

$$\gamma_0 = \sum_j \tau_j^{-1} = \tau_{e-e}^{-1} + \tau_{e-p}^{-1} + \tau_{e-d}^{-1}$$

Lifetime of electron scattering processes is denoted by τ. Electron surface scattering should be included in the above equation for smaller nanoparticles than mean free path of conduction electrons. Hence, considering the size of the nanoparticle, its radius r can be formalised as

$$\gamma(r) = \gamma_0 + \frac{AV_F}{r}$$

Here, V_F is the velocity of electrons at Fermi energy level and A is the theoretical parameter depends on various scattering processes. This results in the accurate determination of 1/r of the plasmon bandwidth as a function of particle size.

In our case, we are working with gold nanospheres and gold nanorods. By varying the size and size of the particle, the electronic and optical properties can be tuned. In gold nanospheres, the phenomenon of surface plasmon resonance was seen. The absorption of the light in a spectrum was observed at ~525 nm. The SPR wavelength in an absorption spectra shifts to longer wavelength with increase in particle size. Similarly, colour of the solution will also change as the size and spectra shifts. Hence, we can vary tune the SPR by changing the size and shape of such nanoparticles for desired optical properties.

In gold nanorods, two LSPR peaks corresponding to transverse and longitudinal modes of electron oscillation were observed. This is mainly due to the anisotropy morphology of the nanorods. In the experimental chapter, FESEM and the absorption spectra of solution of gold nanorods will be presented.

1.2 Quantum Confinement of semiconductor nanoparticles

Many peculiar phenomena were observed when size of the particle is reduced. There are two materials which have energy band gap i.e. semiconductors and insulators. The band gap of semiconductor materials varies with change in the size and shape of the materials. When light is incident with energy equal to the band gap energy, valence band electron get excited to conduction band in a semiconductor material leaving a hole in valence band. A hole is defined as a positively charged particle which is referred as electron absence from the valence band. Due to such electron transition between valence band and the conduction band, electron-hole pair is formed know as exciton. There exists a Coulomb force between two oppositely charged particles with +e and –e at distance of r from each other, then the coulombic force will be stated as

$$F = -\frac{ke^2}{\epsilon r^2}$$

where ϵ is the dielectric constant of the semiconductor material and k is the universal constant.

There are two types of excitons depending on the semiconductor material properties:

a) Frenkel excitons:

   The coulomb interaction between a hole and an electron will be strong, if the semiconductor materials have the small dielectric constant. Thus, in turn exciton have the same order as the unit cell size resulting the lattice constant and the diameter of exciton became comparable. Such Frenkel exciton were observed in alkali halide crystal having a typical binding energy on the order 0.1 – 1 eV.

b) Wannier-Mott excitons:

   When the dielectric constant is large in semiconductor material, the coulomb interaction between a hole and an electron is reduced due to electric field screening. Hence the diameter of excition are larger than the lattice spacing of a unit cell. Such excitons have a binding energy typically on the order of 0.01 eV (which is less than binding energy of hydrogen atom).[4]

   Niel Bohr explain hydrogen atom using Rydberg formula and positronium has bound state energies given by Rydberg formula. Positronium is an atom formed when an electron and positron combines together. The bound state energy can defines as

$$E = -\frac{e^2}{8\pi\epsilon_0 r_{bohr} n^2} = -\frac{6.8}{n^2}\ eV$$

where Bohr's radius is defined as

$$r_{bohr} = \frac{4\pi\epsilon_0 \hbar^2}{m_0 e^2} = 5.29177 \times 10^{-11}\ meter = 0.0529\ nm$$

ϵ_0 denotes the dielectric constant of free space and m_0 represents the mass of electron, Also, n is the quantum number where n = 0, 1, 2, 3,….. ∞.

When the size of the quantum dot is smaller than Bohr radius, then confinement occurs leading to a transition from continuous to discrete energy levels. Also when there is a change in atomic structure due to the influence of length-scale (~1-25 nm) in the energy band structure, quantum confinement occurs in a semiconductor material.[1]

When the electron is confined to few nanometers (nano-material), the spatial extent of the wave function of the electron is comparable to the size of entrapment/material. The electrons experience this constrain of length or boundary and modulate their energy in retaliation to the size constrain. This results into modifying the electrical and optical properties of such material. This phenomenon is called as quantum-size effect. In semiconductors, the effect gains significance near the particle dimension of semiconductor is approximately equal to the bulk surface. One can study and understand quantum confinement with the Bohr exciton radius - a parameter dependent on the size of the material. Thus, the optical absorption and emission profiles can be tuned by quantum size-effect. When nanoparticle size is decreased, the absorption profile gets blue-shifted due to the confinement.[5]

In our work, we study the absorption profiles of CdTe/ CdSe QDs. Due to quantum confinement, CdTe/ CdSe QDs shows tunable emission properties. Different QDs sizes emits light with corresponding wavelength is the reason behind the quantum confinement. The absorption and emission spectra of CdTe/ CdSe QDs will be shown in the experimental chapter.

1.3 Bulk Properties of the materials:

1.3.1 Gold

Gold is a noble, malleable and ductile metal. It is one of the densest metal on the earth after Osmium. In periodic table, it is a group 11 element which comes under transition metals. Gold has a face centered cubic lattice (FCC) crystal structure.

Property	Value
Electronic configuration	$[Xe]4f^{14}5d^{10}6s^{1}$
Atomic number	79
Atomic weight	196.86 g/mol
Density	19.30 g/cm^3
Boiling point	2970° C
Melting point	1064° C
Lattice constant	408 pm
Atomic radius	144 pm
Electrical resistivity	22.14 nΩ m

1.3.2 CdTe

CdTe is a direct band semiconductor material among II-VI compound crystals. CdTe crystal crystallises into cubic (zinc blend) structure however it crystallises into hexagonal (wurtzite) structure when it's in thin films.[6]

Property	Value
Molar mass	240.01 g/mol

Boiling point	1050 °C
Melting point	1041 °C
Density	5.85 g/cm^3
Band gap energy	1.5 eV (at 26.85 °C)
Lattice constant	648 pm (at 26.85 °C)

1.3.3 CdSe

CdSe is the n-type semiconductor among II-VI compound crystal. CdSe crystallises into three forms i.e. sphalerite (cubic), wurtzite (hexagonal) and rock-salt (cubic). Upon slight heating sphalerite structure (unstable in nature) of CdSe converts to wurtzite while the rock-salt structure is observed under high pressure.[7]

Property	Value
Molar mass	191.39 g/mol
Melting point	1268 °C
Density	5.816 g/cm^3
Band gap energy	1.74 eV

1.4 Exciton-Plasmon interaction:

As discussed in the above sections, in metal nanostructures we can tune the absorption and scattering resonances because of the surface plasmon excitations.[8] Whilst in semiconductor nanostructures emission and absorption properties can be controlled. If we were to composite hybrid material by interacting metal with semiconductor, many unique properties can be emerged. Both the nanomaterial in our work is synthesized such that we can tune the optical excitations to resonate with each other. This in result may give rise to coupled excitation which we may have not seen before just by bringing the metal and semiconductor nanostructures in close proximity.[9]

Chapter 2: Experimental techniques

In this chapter, we discuss the methods used to fabricate gold nanospheres, gold nanorods and cadmium telluride quantum dots via colloidal method. Also, we describe how the samples were prepared for the exciton-plasmon interaction for experiments with photoluminescence and time-correlated single photon counting.

2.1 Synthesis of gold nanorods

There are two approaches i.e., top-down and bottom-up to prepare gold nanorods. In the top-down approach, Au NRs are synthesised using a combination of gold deposition and lithography processes whereas bottom-up approach uses wet-chemical, microwave assisted, photochemical reduction, solvothermal and sonochemical methods. In our work, a soft-template based seed-mediated wet-chemical growth method is implemented.[10] The high yield, monodispersity of Au nanorods synthesised at optimum room temperature is the main advantage of this method.[10]

2.1.1 Materials

Cetyl trimethyl ammonium bromide (C TAB), Gold chloride hydrate ($HAuCl_4.3H_2O$), Silver nitrate ($AgNO_3$), Benzyl dimethyl hexadecyl ammonium chloride (BDAC) and Ascorbic acid were bought from Sigma-Aldrich. Sodium borohydride ($NaBH_4$) was purchased from SRL Chemicals Pvt. Ltd, Andheri, India. All chemicals were used without further purification. De-ionized water was used throughout the experiments.

2.1.2 Procedure

In a typical reaction, firsts step is to prepare the 'seed solution'. CTAB (0.2 M, 5 ml) and HAuCl4 (5 × 10−4M, 5 ml) were mixed and gently stirred. Ice-cold NaBH4 (0.01 M, 0.6 ml) were freshly prepared and added to the mix, followed by vigorous stirring for two to three minutes. This turn the solution into brownish-yellow colour. The second step, 'growth solution' involves CTAB (0.2 M, 2.5 ml) solution which acts as a surfactant and BDAC (0.15 M, 2.5 ml) as another surfactant. To this solution, AgNO3 (4×10^{-3} M, 0.2 ml) was added. Then $HAuCl_4$ (0.01 M, 5 ml) solution was added with gentle stirring resulting the solution into

golden-yellowish colour. Then, ascorbic acid (0.0788 M, 0.07 ml) was added with gentle mixing, which results the solution colourless. Lastly, 12 µl of the seed solution was added to the growth solution, and the solution was kept undisturbed at RT for 12 hours. A dark-magenta colour of the growth solution showed the development of gold nanorods. The schematic procedure is shown with the help of a flow chart in the figure below.

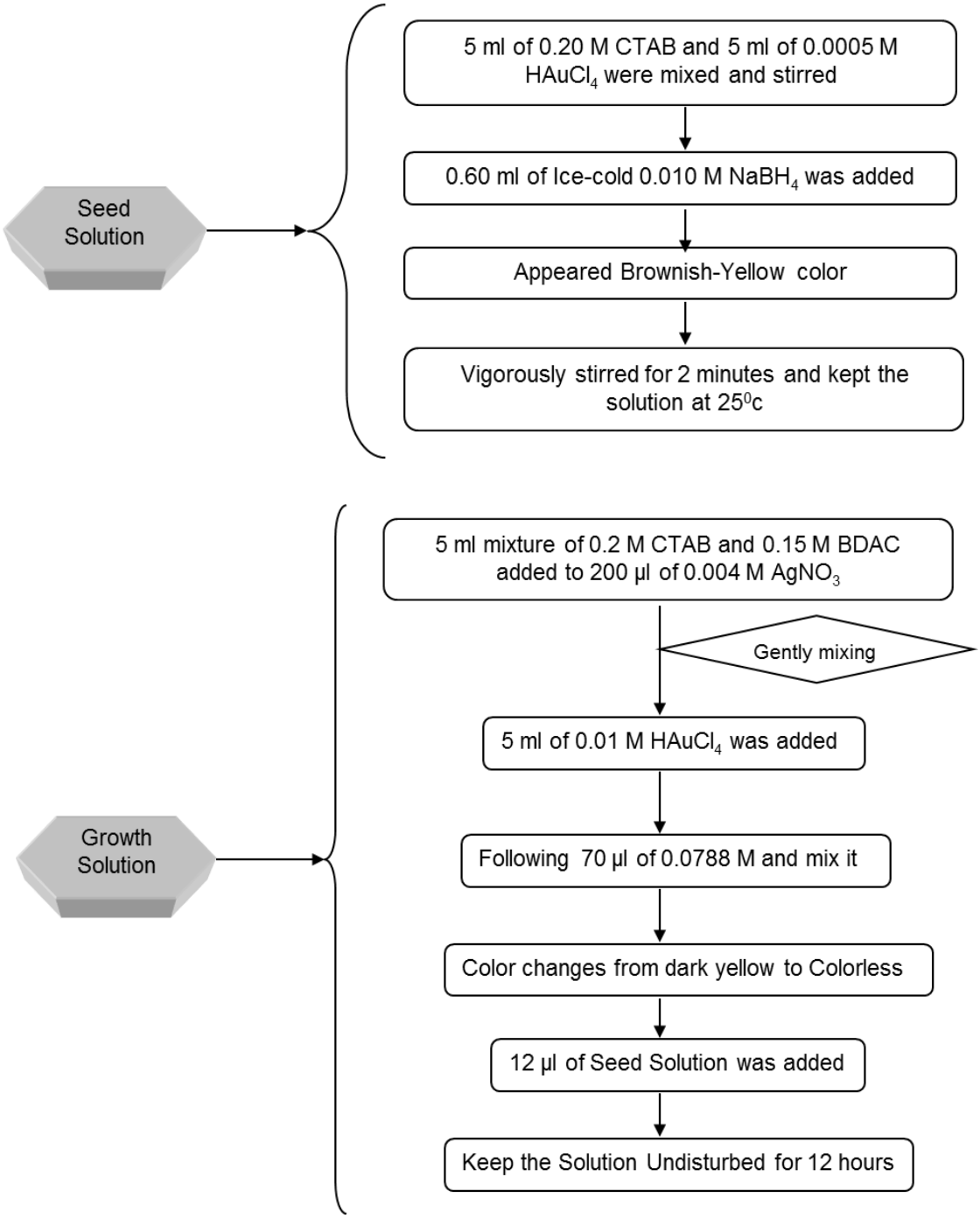

Figure 2: *Schematic flowchart of the two-step seed-mediated synthesis of gold nanorods*

2.2 Synthesis of gold nanospheres

Over the period of the first synthesis of gold nanospheres by Turkevich et al,[11] many synthesis strategies came along to obtain uniform shape and size of gold nanospheres. In our work, seed-mediated synthesis method was used by Puntes et al.[12] Citrate-stabilized gold nanospheres was synthesised ranging from 22 nm to 200 nm.

2.2.1 Materials used

Gold chloride hydrate ($HAuCl_4.xH_2O$) was bought from Sigma-Aldrich and Trisodium Citrate was purchased from Alfa Aesar. All chemicals were used without further purification. De-ionized water was used throughout the experiments.

2.2.2 Procedure

In a typical reaction, Au seed were synthesized by adding HAuCl4 (25mM, 1ml) into Sodium Citrate (2.2 mM, 150 ml) at 100°C. During the reaction, observance of colour change from yellow to soft pink. The reaction mixture was cooled down to 90°C. Then HAuCl4 solution (25 mM, 1 ml) and sodium citrate solution 60 mM, 1ml) were consecutively added with a time delay of approximately two minutes. Every 30 minutes (repeating the process), 2 ml aliquot were taken out for further characterization and experiments.

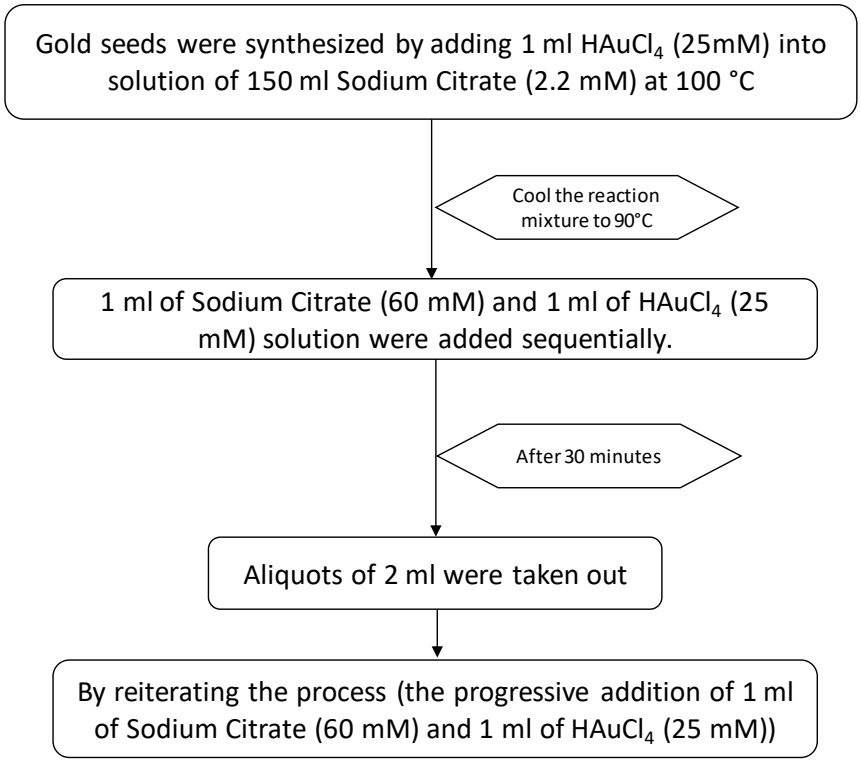

Figure 3: *Schematic flowchart of the two-step synthesis of gold nanospheres*

The schematic workflow of the experiment was shown in the figure below[12]:

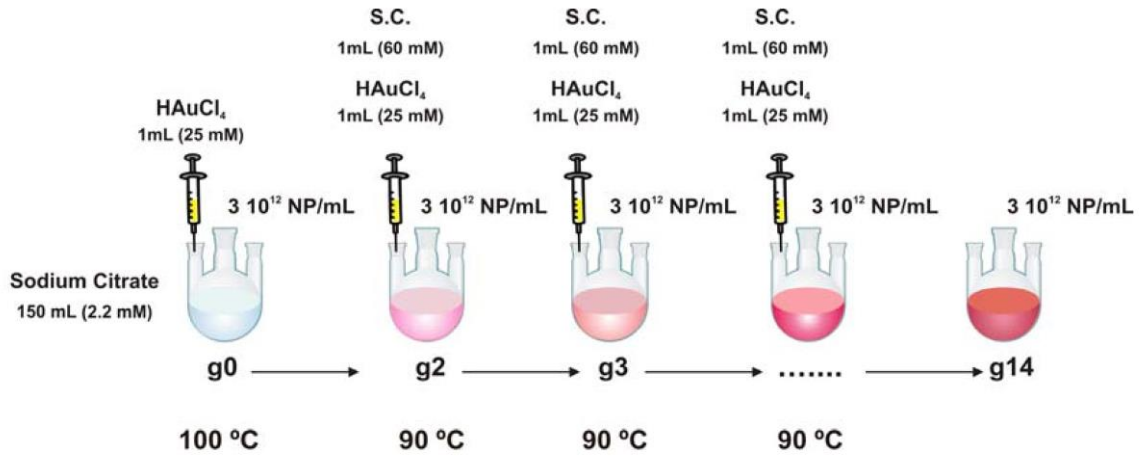

Figure 4: *Schematic illustration of the two-step synthesis of gold nanospheres*[12]

2.3 Synthesis of CdTe QDs

Given two approaches for CdTe QDs i.e., aqueous and non-aqueous medium synthesis. We preferred aqueous synthesis of CdTe QDs since we have to further do the experiments with wet chemically synthesised gold nanorods and spheres. Facile synthesis method was reported by Chen et al for CdTe QDs.[13]

2.3.1 Materials

Cadmium acetate ($Cd(Ac)_2 \cdot 2H_2O$), L-cysteine ($C_3H_7NO_2S$) and Sodium Tellurite (Na_2TeO_3) were bought from Sigma-Aldrich. Trisodium Citrate was bought from Alfa Aesar. Sodium Borohydride ($NaBH_4$) was bought from SRL Chemicals Pvt. Ltd. Andheri, India. De-ionized water was used throughout the experiments. All chemicals were used without further purification.

2.3.2 Procedure

Typically, L-cysteine (67.8 mg) was transferred to a solution containing $Cd(Ac)_2$ (96.5 mg) with de-ionized water (150 ml) under N_2 atmosphere. NaOH (O.5 M, 3 ml) was added to the mixture for adjusting its pH to 11.0. Then, trisodium citrate (223.5 mg) and Na_2TeO_3 (17.9 mg) were added, correspondingly. Following this, $NaBH_4$ (16.5 mg) was added and fizzed the whole reaction solution by nitrogen N_2 for around 15 min. Lastly, 25 ml of the solution was used for further reaction in another reaction-flask at 160°C till 320 minutes.

Aliquots were taken during reaction at different times and checked instantly under UV lamp. The schematic synthesis of CdTe QDs were given as follows:

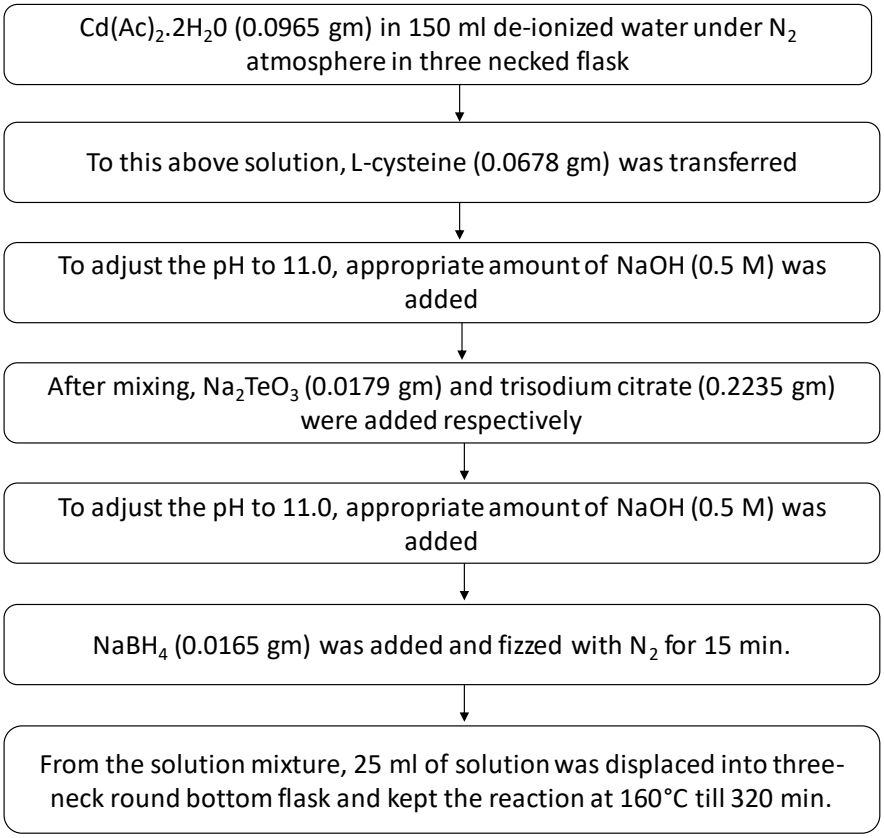

Figure 5: *Schematic flowchart of working synthesis of L-cysteine capped CdTe QDs*

During the reactions, sodium borohydrate reduces TeO_3^{2-} to Te^{2-}, and the fresh Te^{2-} reacts with Cd^{2+} to yield CdTe. To avoid the deposition of cadmium tellurite ($CdTeO_3$), citrate is added.[14]

Here are the chemical reactions proceeded during the reaction:

$$4\,TeO_3^{2-} + 3\,BH_4^{1-} \rightarrow 4Te^{2-} + 3BO_2^{1-} + 6H_2O$$

$$CdR + Te^{2-} \rightarrow CdTe + R \qquad \text{R is cysteine group}$$

2.4 CdSe QDs

Non-aqueous CdSe QDs were prepared using a wet-chemical method by a collaborator at University of Pune. Phase change from chloroform to water was done to perform experiments with water based gold nanorods and gold nanospheres. Please note, this synthesis and characterization was done at University of Pune by a collaborator.

2.5 Analysis Techniques

2.5.1 UV-Vis Absorption

Electromagnetic wave comprises of packets of photons which carry energy. The amount of energy carried by a photon is dependent on the frequency of the electromagnetic radiation. Atoms comprises of electrons which occupy discrete energy levels within the atom. Photons (UV-Visible) which have energy equal to the energy gap between two energy states can excite electrons to higher states. In a bulk material, the molecules have the freedom to rotate and vibrate, the energy with which these modes can be excited like typically in the Infrared radiation of the electromagnetic spectrum. Thus, using light as a probe one can characterize physical properties of a material. UV-Vis-IR spectroscopy is based on this principle. By modulating the incident energy of the incoming radiation one can probe electronic, vibrational or rotational excitations. We use spectroscopy to characterize the optical properties of nanoparticles. The spectrum and thus the properties depends on the shape and size, concentration and refractive index of the nanoparticle surface.

This technique measures the absorption and scattering of light of the sample as a function of its wavelength. Basically, a parameter named extinction co-efficient defined as the sum of the scattering and absorption co-efficient (derivative from Mie's theory). This we have discussed in the chapter 1 in details.

In a typical experiment, liquid samples in a quartz cuvette are placed between the source and a photodetector. A D_2 lamp ($\lambda \ll 320\, nm$) as a UV source and a tungsten lamp for the vis-NIR regions were used in the instrument. A monochromator is used to tune the incident wavelength which passes on to the sample stage through mirror optics. A PbS ($\lambda > 860\, nm$) collects the transmitted beam from the sample which is further characterised and displayed by the default software on a computer. Further, the data is plotted as extinction as a function of wavelength.

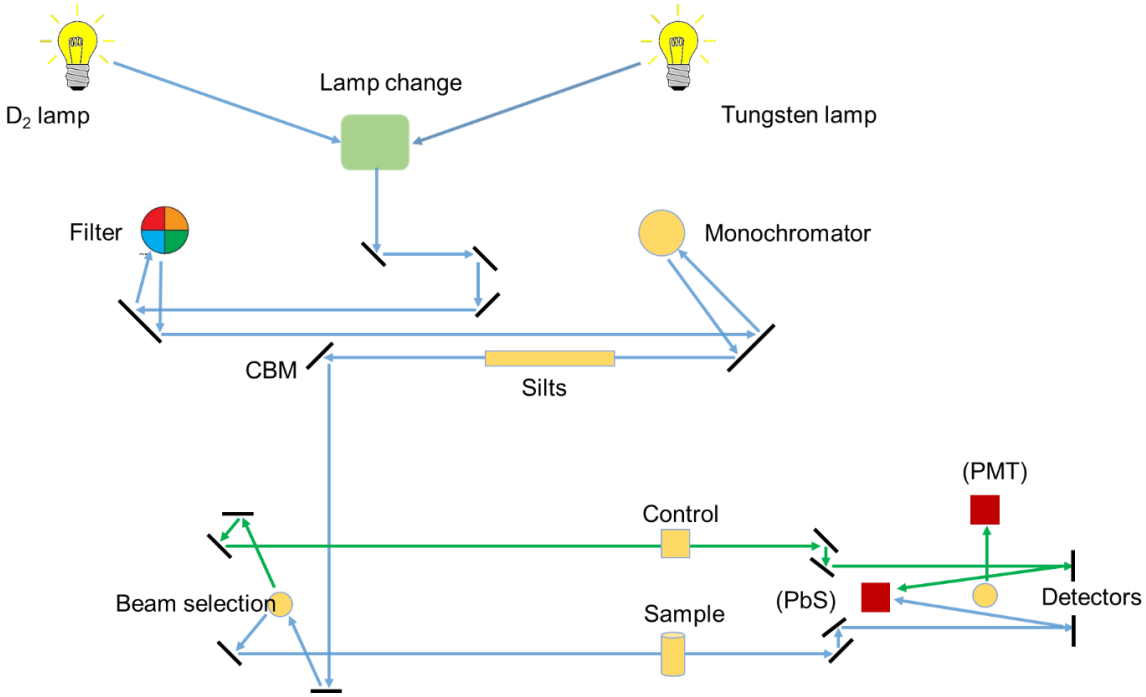

Figure 6: *Illustration of UV-Vis spectrometer*

2.5.2 Field-emission Scanning Electron Microscope

The Rayleigh criteria defines a classical limit on the resolution with which one can image an object using a microscope. To image any object to a precision in length of order l, the wavelength of light used to image this object must be of the order of l. Thus, in order to measure changes at a length scale of a few nanometers the wavelength of light source must be of this order. From the principle of wave-particle duality we have the liberty to choose if we probe the object at this scale with an electromagnetic radiation or an electron. The Abbe's formula limits the use of electromagnetic radiation to image small objects. Thus, we use electrons which help us to resolve objects to a sub-micron level, giving this microscopy the name 'Field Emission Scanning Electron Microscope' (FESEM). Another advantage of using electrons is that by varying their energy we vary their wavelength and thus the resolution with which we can film an image.

We know that electrons are emitted from the surface of metals if the temperature is high enough (Thermionic emission). In a scanning electron microscope, we use a hot tungsten/zirconium oxide as the source of electrons. However, to image at sub-micron level the energy of electron has to be sufficiently boosted. To do so a series of high voltage gradients are used to accelerate

the electrons emitted from the cathode to higher energies. FESEM machines are capable of accelerating electrons to 3-30 KeV (3-5 nm) resolution. Next, the electron beam is collimated to ensure high flux of electrons to sample the image using magnetic lenses. The beam of electron which bombards the sample is called the primary beam and in the process, produces secondary electrons from the sample and back scattered electrons. We also have electromagnetic radiation in UV-visible also. The secondary electrons bear the imprint of the sample surface under investigation and are detected by the in-lens annular SE detector, which used the energy and angle information to get an electronic signal mapped these to the solid surface. This signal is amplified and generated as an FESEM image.

All results presented in our study are recorded by a Zeiss Ultra-Plus Field Emission Scanning Electron Microscope. The schematic image of a FESEM is shown in the figure below:

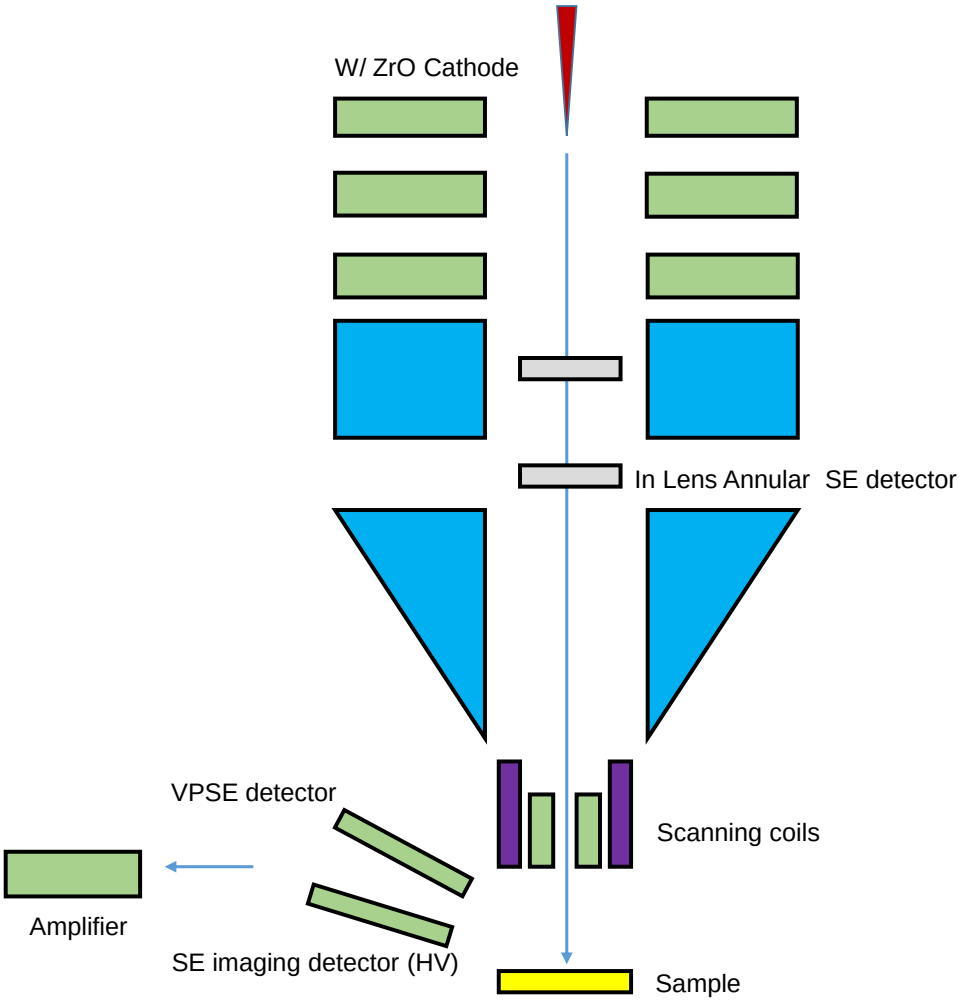

Figure 7: *Illustration of FESEM*

2.5.3 Photoluminescence Spectroscopy

Photoluminescence is used to investigate the energy levels of a semiconductor quantum well structure. Photoexcitation of electrons is done by a laser in GaAs semiconductor. These electrons start emitting luminescence when they get de-excited spontaneously since such spectrometer is used to analyse the luminescence. The energy levels of a semiconductor is represented by the peaks shown in the spectra which we will see in Chapter 3.

Semiconductors have band-gap energy. Basically, some electrons in solids are not strongly attached to atoms, they can jump from one atom to other atom. These electrons are attached to atoms in different amounts. This results into band gap to have different energies.[1]

Electron with low energy is referred as valence electrons and electron with high energy is referred as conduction electrons. But there is a gap between conduction electron state and valence electron state. In normal condition, electrons are not allowed to hold energies between conduction band and valence band. Photons can excite electrons to conduction band from valence band through the forbidden energy gap if they have greater energy that band gap energy. In this process, the excess energy of electrons loses, then comes to rest in the conduction band at very low energy. The electrons fall back to the valence band. At this point the energy of emitted photons measures the band gap energy. This process is called photoluminescence.

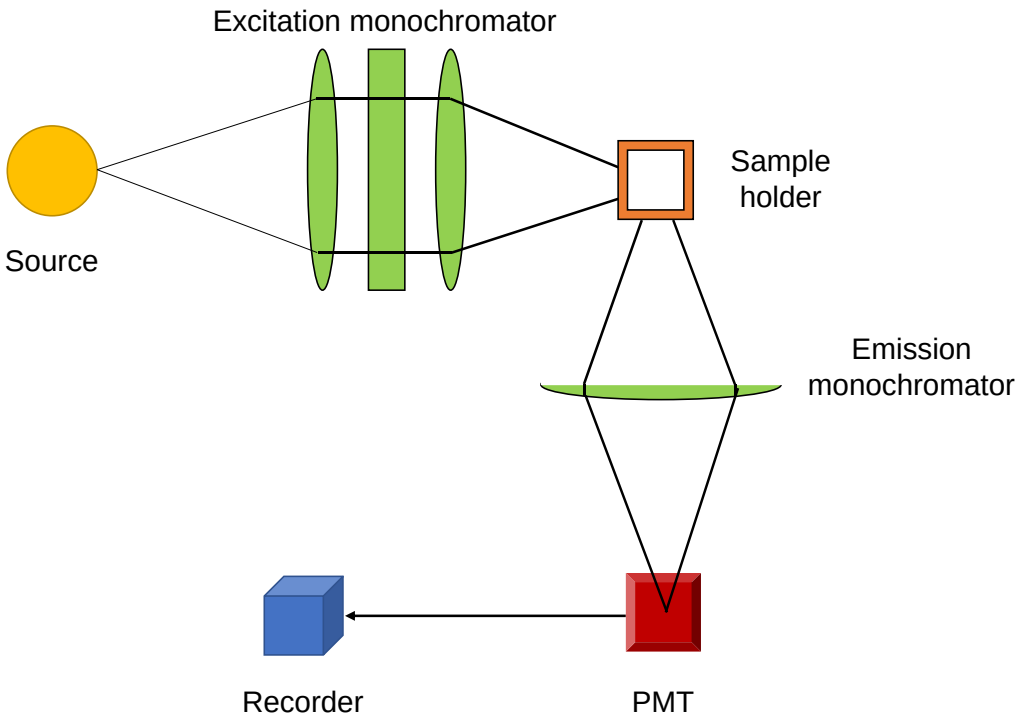

Figure 8: *Illustration of photospectrometer*

2.5.4 Time-correlated Single Photon Counting

Photons illuminated over a sample of molecules excite the electrons from the ground state to the higher excited states. These excited electrons relax back to lower energy states emitting photons of the characteristic energy corresponding to the difference in energy of the two states. The rate of decay on the number of electrons from the excited state is proportional to the number of possible pathways (both radiative and non-radiative) for the decay. In photoluminescence, we measure the light and intensity of the emitted radiation. Lifetime of excited state is inversely proportional to the rate of decay. The fluorescence lifetime imaging (FLIM) setup is used to measure the lifetime of the excited state molecules.

The FLIM setup comprises of a laser light source which illuminates the sample. The florescent light emitted from this sample is received by a single photon counting detector. The time correlated single photon counting (TCSPC) correlates the photons from the laser source and the single photon counting detector. TCSPC detector correlates the single in frequency and time domain. In frequency domain, the phase difference between the two sources provides the information about the lifetime of the molecule. In time domain, information about the

correlation time between the photons from the laser source and the photo luminescent sample is accumulated over time. The following process is stochastic, by plotting a binned histogram of the correlation times, we can estimate the decay rate and thus the lifetime of the sample under investigation.

All results presented are acquired from the spectrometer FLS980 Series Edinburgh TCSPC UV-NIR fluorimeter for studying Steady State and Time Correlated Single Photon Counting (TCSPC) for decays in picoseconds to microseconds range at IISER Pune.

Chapter 3: Results and Discussion

This chapter illustrates the characterization of synthesized gold nanospheres, gold nanorods, CdTe QDs, CdSe QDs using UV-Vis absorption spectroscopy, FESEM images. Also, the experiments with Photoluminescence and TCSPC.

3.1 Colloidal gold nanospheres

Uniform colloidal gold nanospheres (Au NSs) were synthesized using a seeded growth route described in the Chapter 2. Citrate-stabilized gold nanospheres were fabricated using two-step seeded growth method is implemented.

This strategy is constructed on the traditional Turkevich-Frens reaction system. It emphases on the inhibition of secondary nucleation throughout the homogeneous growth period, letting the coalescence of the nuclei into bigger particles via the surface-catalyzed reduction of Au^{3+} to Au^{0} by sodium citrate.[15]

The UV-Vis absorption spectrum of a gold nanospheres solution is shown in the figure. In chapter one, we mentioned spherical gold nanoparticles show single surface plasmon resonance peak whereas gold nanorods show two peaks corresponding to transverse mode and longitudinal mode of LSPR.

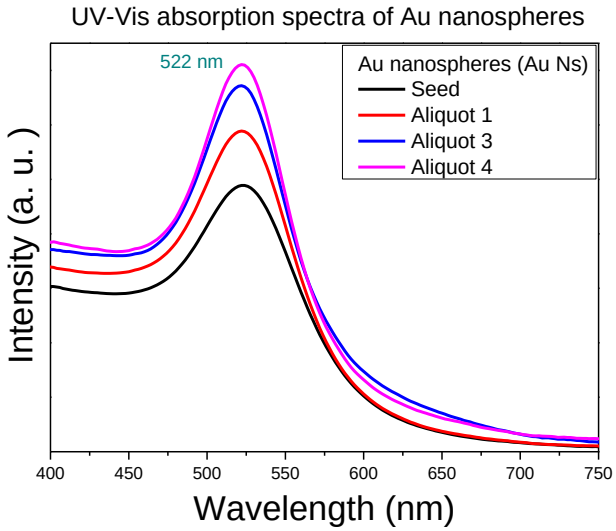

Figure 9: *UV-Vis absorption spectra of gold nanospheres*

FESEM was used to find out the size of the gold nanospheres which is observed to be 22 nm as shown in the figure.

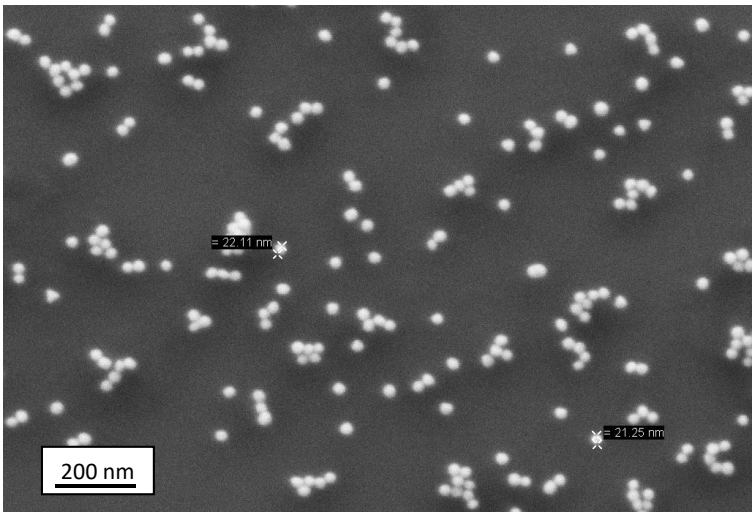

Figure 10: *SEM micrograph of gold nanospheres*

3.2 Colloidal gold nanorods

Synthesis of uniform colloidal gold nanorods using a two-step seed-mediated growth method described in the Chapter 2. The final colour of the solution looks maroon as shown in the below figure.

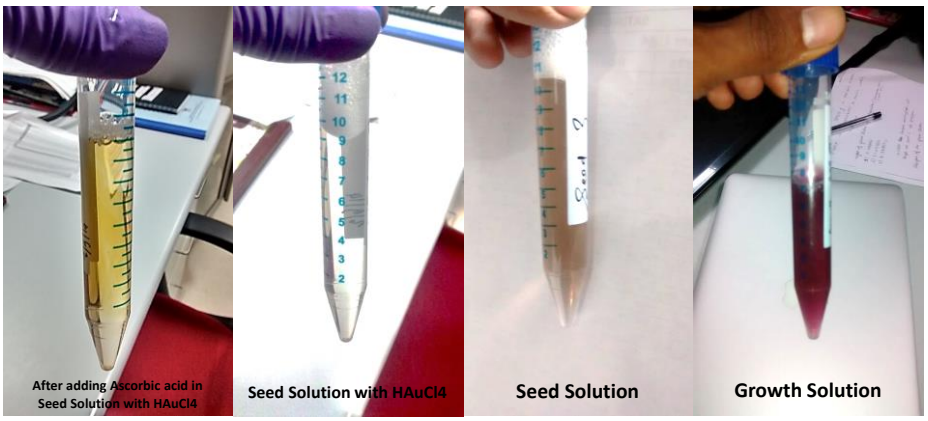

Figure 11: *Colour of gold nanorods solution at different steps*

The UV-Vis absorption spectrum of a gold nanospheres solution is shown in the figure. In chapter 1, we mentioned gold nanorods show two peaks corresponding to transverse mode and longitudinal mode of LSPR. This was clarified by Mie-Gans theory and this resulting peaks appears due to the presence of anisotropy in gold nanorods.

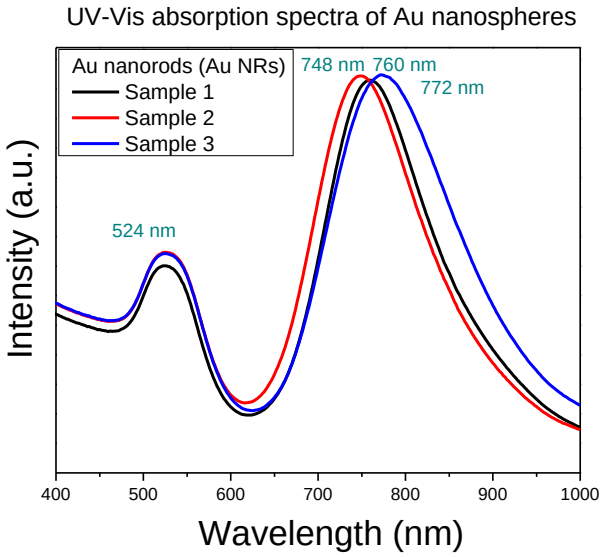

Figure 12: *UV-Vis absorption spectra of gold nanorods*

From FESEM images, the gold nanorods morphology was confirmed. It was observed that the length of gold nanorods were 50 nm and width 12 nm.

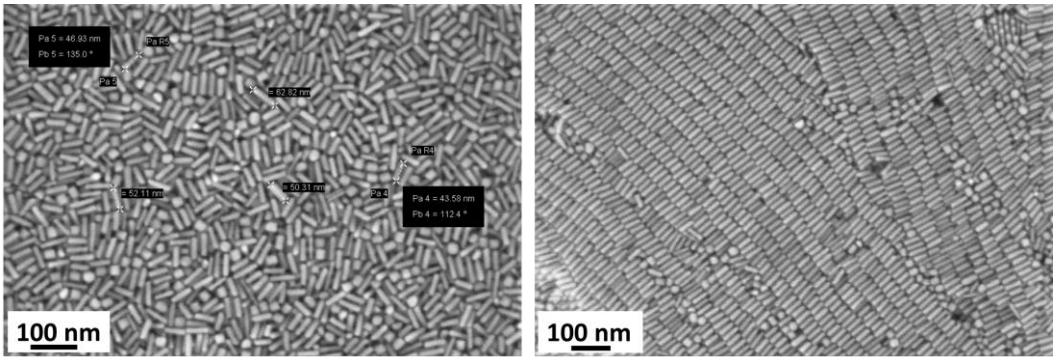

Figure 13: *SEM images of gold nanorods*

3.3 CdTe quantum dots

As discussed in Chapter 2, CdTe quantum dots were prepared in a water-soluble medium. In our case, as we study the interaction between exciton-plasmon, water-soluble method is used for all the synthesis. This is the key factor in terms of miscibility to do the experiments in the same medium.

Since gold nanospheres and gold nanorods were synthesized in aqueous medium, we choose the synthesis of CdTe QDs in aqueous medium. In Chapter 2, as explained, during the reaction course, we took aliquots in between to acquire various sizes with emission at different wavelength. The number of aliquots were checked at the time under UV light illumination showing colours as shown in the figure below. Notably, the CdTe quantum dots were L-cysteine functionalized (so thiol group is attached to CdTe) which gives us the advantage of free ammonia group.

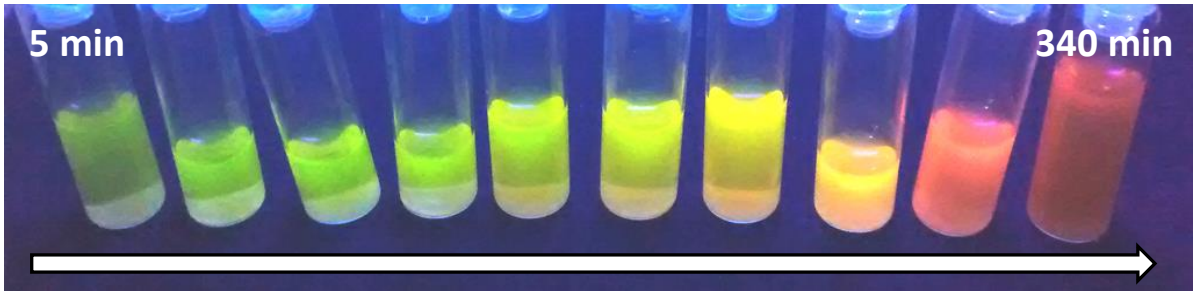

Figure 14: *Under UV lamp exposure, Colours of CdTe QDs aliquots at various time of reaction*

The UV-Vis absorption spectrum of a CdTe QDs solution is shown in the figure. The spectra show the absorption peak at different wavelength as mentioned in the figure ranging from 492 nm to 614 nm. The estimated size of the particles was ~10 nm. But with increase in reaction time, relative red-shift is observed mainly due to the increase in size of the particle.

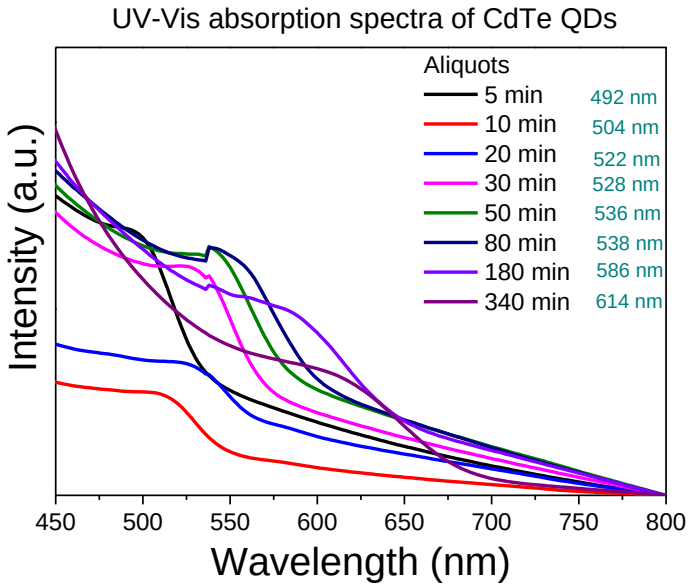

Figure 15: *UV-Vis absorption spectra of different aliquots of CdTe QD*

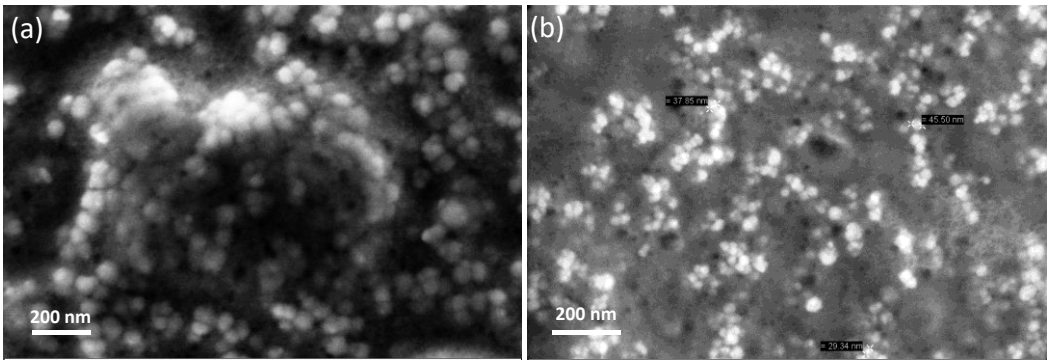

Figure 16*: (a) SEM image of CdTe QDs aliquot at 180 mins (b) SEM image of CdTe QDs aliquot at 320 min*

The Figure shows photoluminescence (PL) spectra recorded for various aliquots taken at different times of reaction. Similarly, along the absorption spectra, it was observed that with increased reaction time, emission wavelength of CdTe QDs is shifting towards longer wavelengths. The emission wavelength ranging from 513 nm to 643 nm was seen.

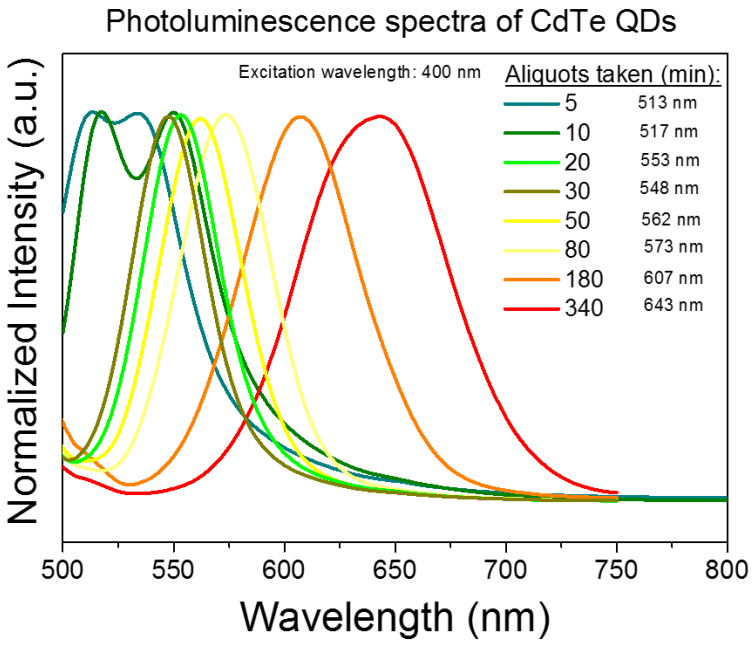

Figure 17: *Fluorescence spectra of CdTe QDs aliquots at different times*

Additionally, we observed increment of Full-Width-Half-Maximum (FWHM) of PL spectra with increased reaction time. This shows that with increase in size emission wavelength has increased which means there is a decrement in band gap energy which approves with the literature discussed in Chapter 1. Since the method of synthesis adopted here is a water-based route, not every particle can be of same size. This is due to non-uniformity, different sizes of quantum dots resulting different band gap energies thus different emission profiles and hence the convolution of all such emission profiles might have resulted into broadened emission spectra. So, for samples with less reflux time, narrower emission profile has been observed while for those with longer reflux time show broader emission profile.

In our experiments, we successfully synthesized thiol-capped CdTe QDs with tunable size-dependent emission from green to red by controlling the refluxing time. Since it is in water-based medium, after a week, CdTe QDs loses their fluorescence properties, we did various synthesis making sure CdTe QDs has desires emission wavelength.

Another analysis for the synthesis of CdTe QDs. The Figures shows as described.

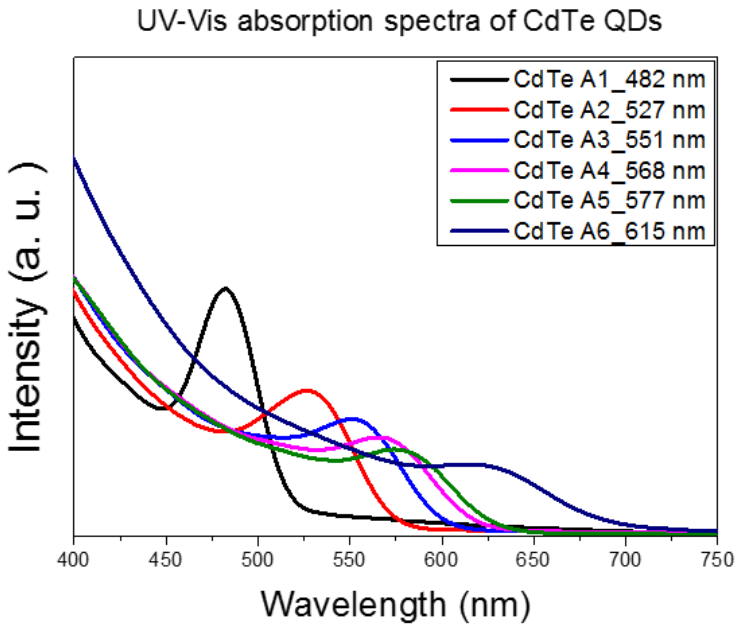

Figure 18: *UV-Vis absorption spectra of different aliquots of CdTe QD (another synthesis)*

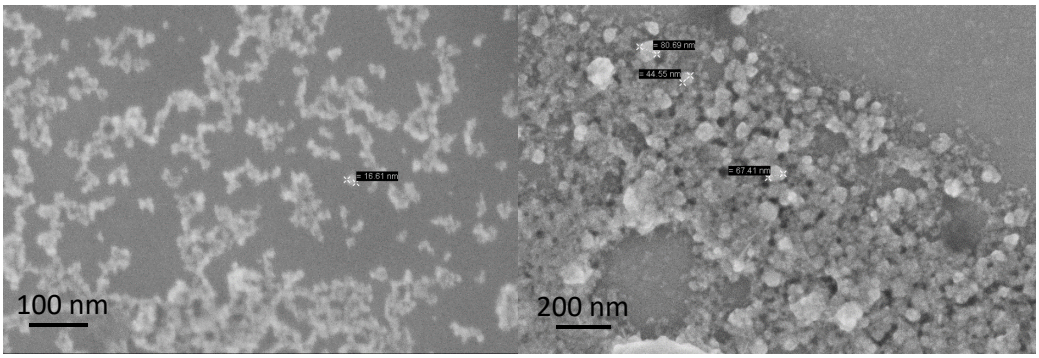

Figure 19: *SEM micrographs of CdTe QDs of aliquot A2*

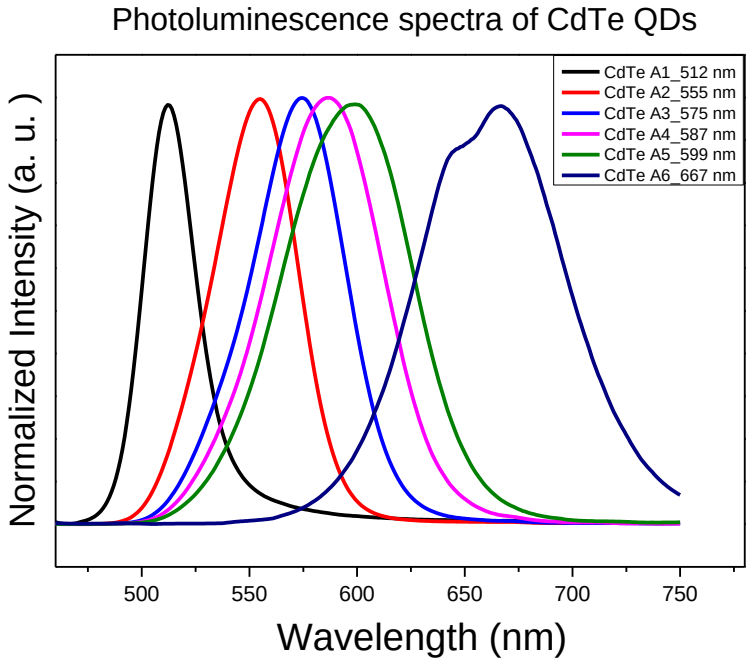

Figure 20: *Fluorescence spectra of different aliquots of CdTe QD*

3.4 Metal-Semiconductor interaction

For interaction of metal with the semiconductor (as in our case gold and CdTe/CdSe), a novel method has been used which has not been published yet.

Earlier in Chapter 2, we talked about synthesized L-cysteine capped CdTe QDs which has free ammonia group after the reaction. In case of gold nanospheres and gold nanorods, by centrifuging the sample we stop the growth and remove excess of ions and surfactant and re-disperse the nanoparticles in distilled water. It is known that amine group has a weak attraction towards gold. Since, CdTe QDs is capped through thiol bond via cysteine, leaving the amine group free, gold nanoparticles can form a weak covalent bond with amine group which might lead to plasmon-exciton interaction.

We also did some experiments with CdSe QDs. As discussed in Chapter 2, CdSe QDs was prepared in non-aqueous medium. Through solvent phase transfer, chloroform to water, was achieved. We were able to perform absorption and emission measurements with CdSe QDs with gold nanospheres.

3.4. 1. CdTe QDs and Au Ns

The UV-Vis spectra of CdTe QDs with the addition of Au NSs were performed as shown in the figure. Au NSs were sequentially added to the fixed solution of CdTe QDs. While doing measurements, dilution of sample solution was done with utmost care for the ease of comparing with emission as well as absorption intensities.

The original CdTe QDs absorption was observed at 510 nm. As the Au NSs amount was increased from zero, the absorption spectra red shift while taking a sharp peak indicating some interaction happening at the time.

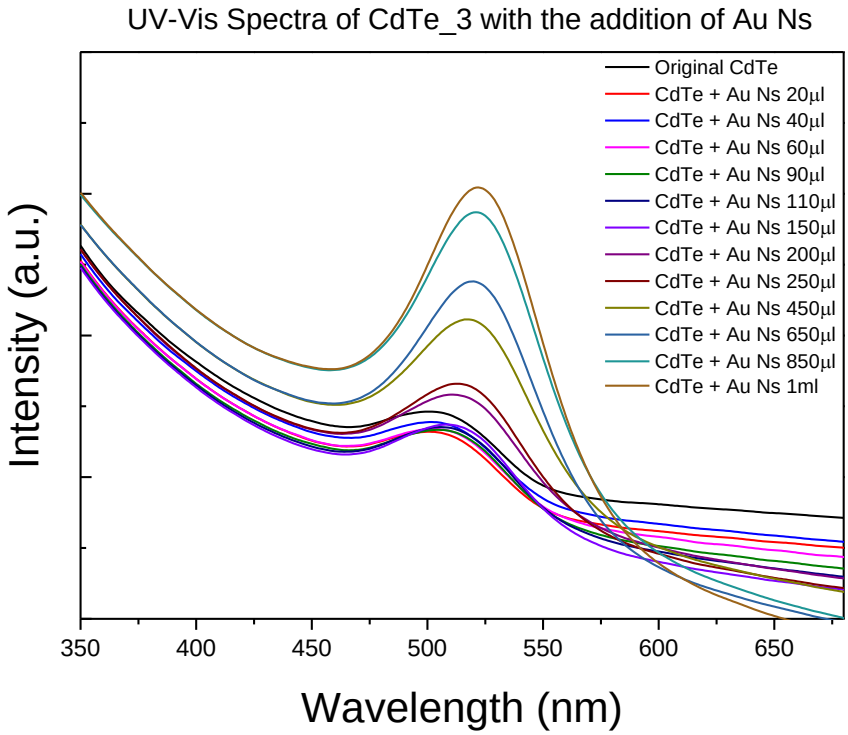

Figure 21: *Absorption spectra of CdTe QD with addition of gold nanospheres*

The PL spectra shows the emission profile with the addition of Au NSs solution. The excitation wavelength of 410 nm was fixed during the measurement. As expected, the emission profile shows decrease in intensity with increasing amount of Au NSs. This is due exciton-plasmon coupling. The following figure shows the emission spectra.

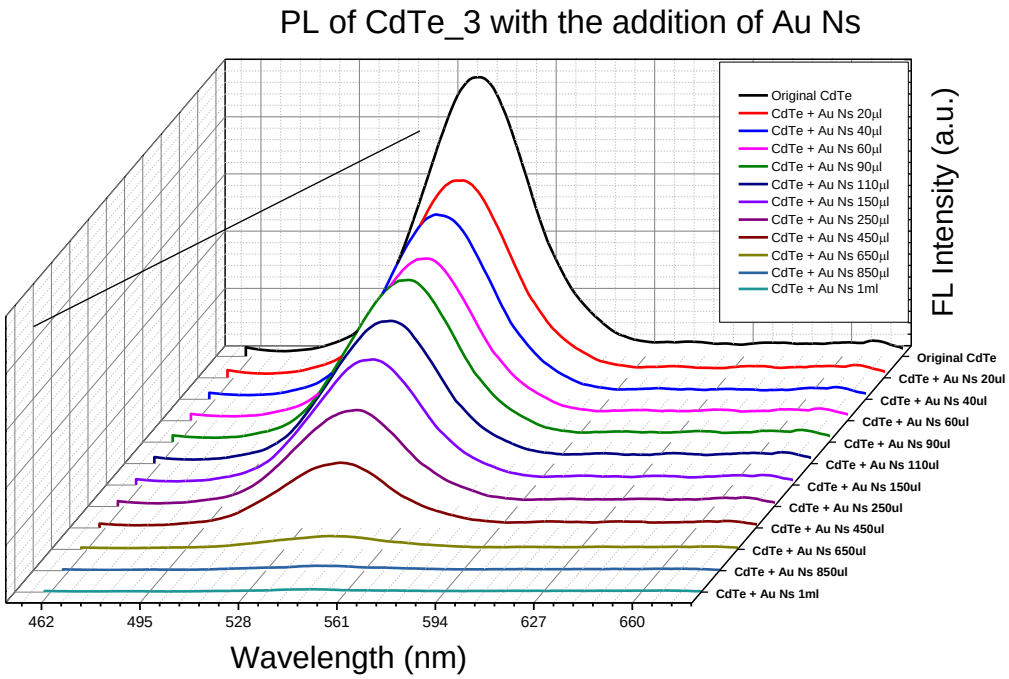

Figure 22: *PL spectra of CdTe QD with addition of gold nanospheres*

To obtain variations in lifetime of different concentration of Au NSs in CdTe QDs solution, Time-correlated single photon counting (TCSPC) was done. The figure below shows the time-resolved fluorescence spectra of CdTe QDs with the sequential addition of Au NSs solution.

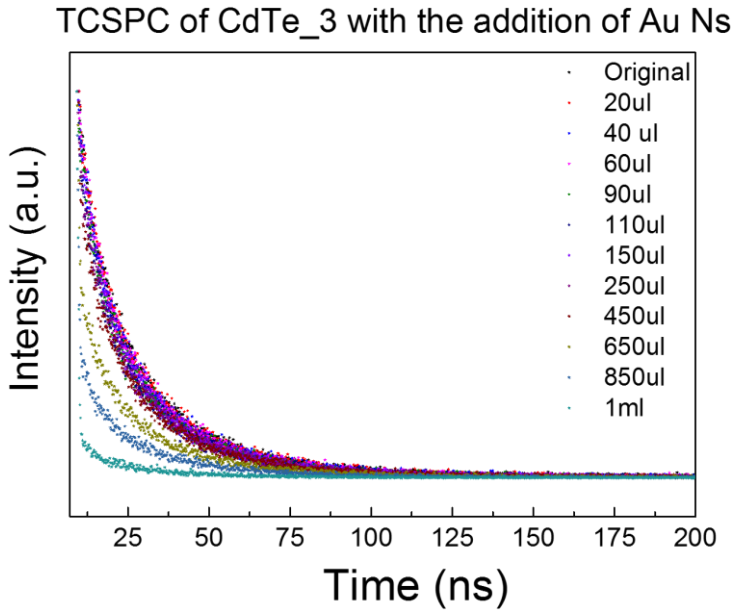

Figure 23: *TCSPC study of CdTe QD with addition of gold nanospheres*

Sample	τ_1(ns)	τ_2(ns)
Original CdTe	22.07	4.92
CdTe + 20 µl Au NSs	22.50	5.89
CdTe + 40 µl Au NSs	22.25	5.92
CdTe + 60 µl Au NSs	22.74	6.47
CdTe + 90 µl Au NSs	21.88	5.04
CdTe + 110 µl Au	20.23	3.98
CdTe + 150 µl Au	21.65	5.60
CdTe + 250 µl Au	19.40	2.90
CdTe + 450 µl Au	18.44	1.41
CdTe + 650 µl Au	17.04	0.64
CdTe + 850 µl Au	17.04	0.55

The individual lifetime was fitted with the double exponential decay function. The results were summarized in the table below.

The fitted model can be stated as:

$$x = x_0 + A_1 e^{-t/\tau_1} + A_2 e^{-t/\tau_2}$$

where $\tau_1$and $\tau_2$are decay constants. Also, $A_1$and $A_2$are pre-factors.

From the table the decay was observed to be decreasing as in tune with the PL study.

3.4.2 CdTe QDs and Au NRs

Similarly, CdTe QDs absorption and emission spectra was recorded with the addition of gold nanorods (Au NRs). As seen in the absorption spectra, with increase in the amount of Au NRs the longitudinal peak started to appear as well as the transverse peak were taking the sharp peak.

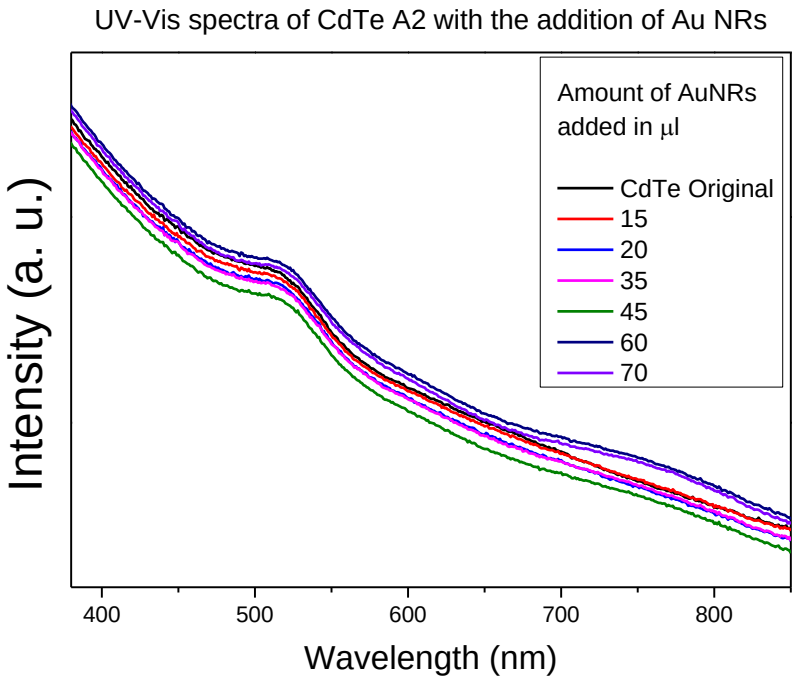

Figure 24: *Absorption spectra of CdTe QD with addition of gold nanospheres*

In case of emission profile, quenching phenomenon was observed indicating exciton-plasmon interaction. The PL spectra was performed as fixed excitation wavelength of 410 nm.

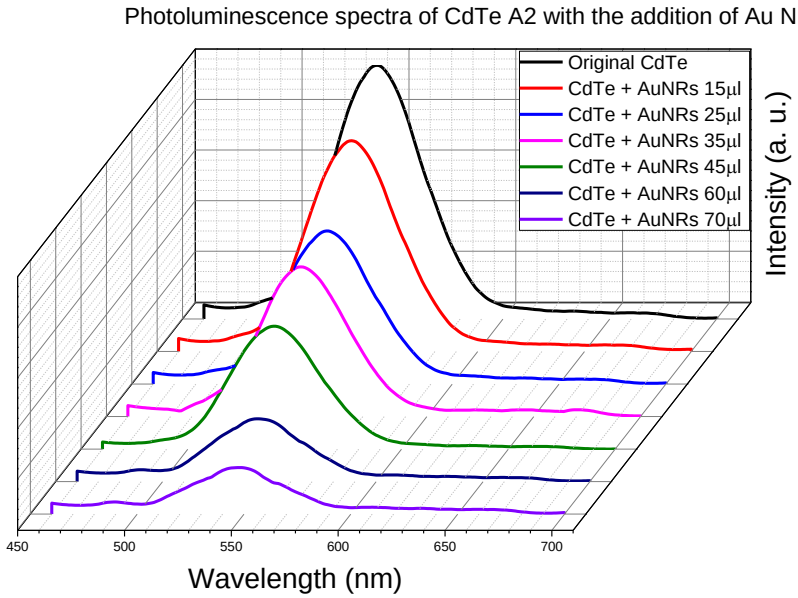

Figure 25: *PL spectra of CdTe QD with addition of gold nanospheres*

The study of TCSPC was done by recording decay lifetime of the samples with the addition of Au NRs. The data of the lifetime decay is summarized in the table below

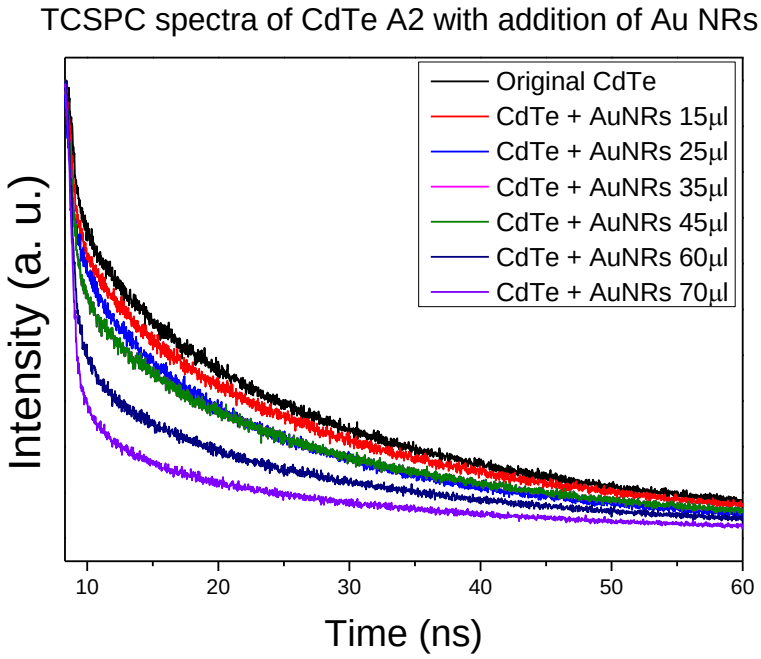

Figure 26: *TCSPC study of CdTe QD with addition of gold nanorods*

Samples	τ_1 (ns)	τ_2 (ns)
Original CdTe	6.99	0.30
CdTe + AuNRs 15µl	2.36	0.22
CdTe + AuNRs 25µl	1.72	0.23
CdTe + AuNRs 35µl	1.87	0.23
CdTe + AuNRs 45µl	1.80	0.23
CdTe + AuNRs 60µl	5.23	0.25

3.5 Additional experiments with CdSe QDs

In chapter 2, we talked about the phase change of CdSe QDs. The figure below shows the UV-Vis absorption spectra of CdSe QDs in both medium showing no change in the absorption wavelength which is recorded at 561 nm.

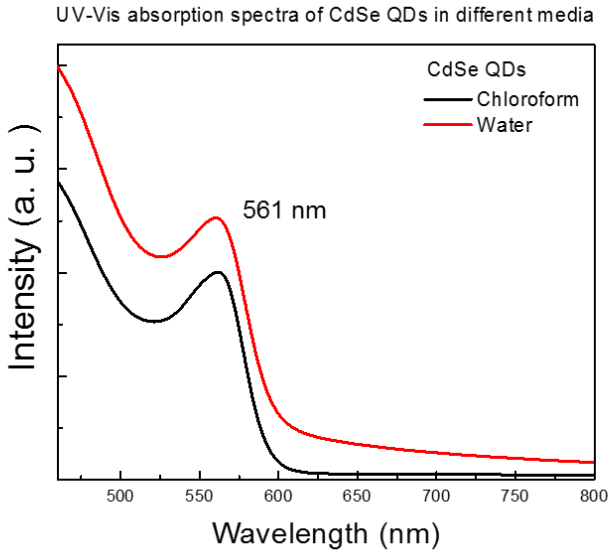

Figure 27: *Absorption spectra of CdSe QDs in two medium*

For the same, PL spectra was also recorded in both media but here the emission profile was red-shifted from 575 nm to 590 nm. The excitation wavelength during the measurement were fixed at 410 nm.

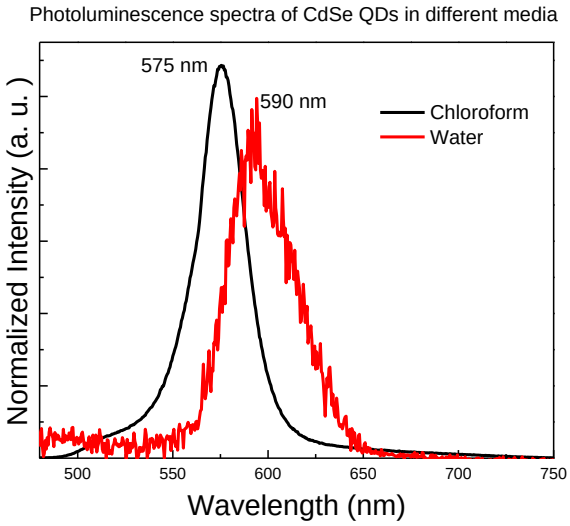

Figure 28: *Emission spectra of CdSe QDs in two medium*

To study the morphology of the CdSe QDs, transmission electron micrographs were done at University of Pune. The observed size of the CdSe QDs were around 2 nm. The figure below shows the TEM images.

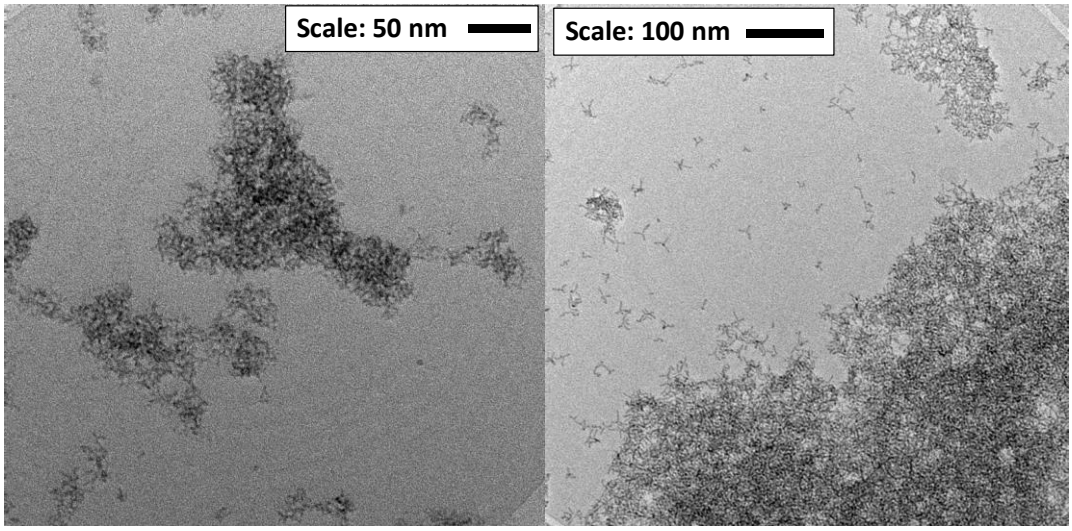

Figure 29: *TEM images of CdSe QDs*

Absorption and emission spectra was recorded with the addition of gold nanospheres. In the absorption profile, blue-shift was observed and increase in the sharpness of peak was seen. The blue shift is indicated in the UV-Vis absorption spectra from 546 nm to 544 nm.

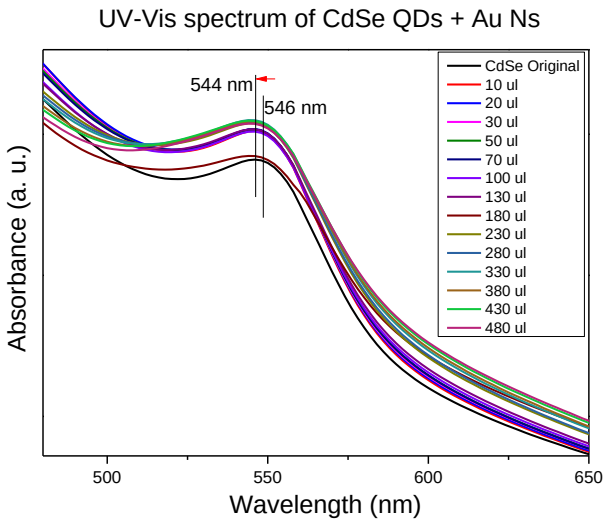

Figure 30: *UV-Vis absorption spectra of CdSe QDs with sequential addition of gold nanospheres*

As expected quenching was observed with increasing amount of Au NSs to the fixed amount of CdSe QDs solution. The PL experiment was done at fixed excitation wavelength of 410 nm. Here we also observe the same phenomena of exciton-plasmon coupling. The figure shows the PL study of CdSe QDs with addition of Au NSs

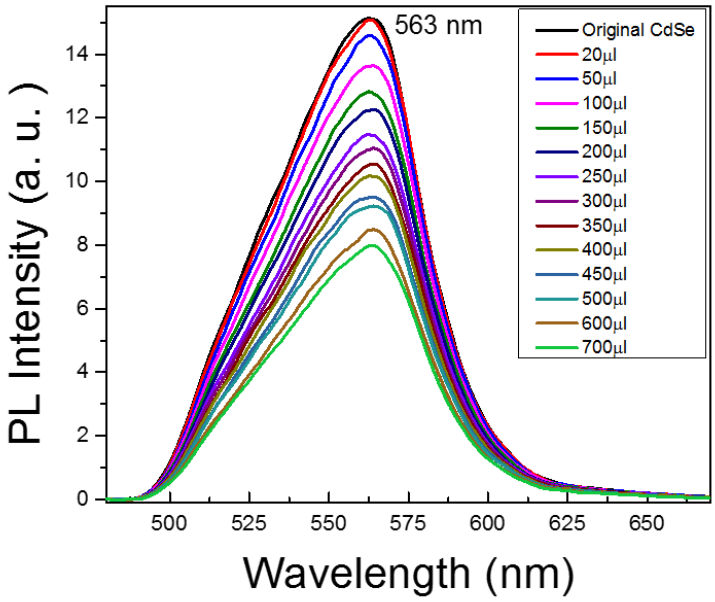

Figure 31: *PL spectra of CdSe QDs with sequential addition of gold nanospheres*

Conclusion

Successful synthesis of colloidal gold nanospheres, gold nanorods, CdTe QDs were done using wet-chemical methods. All synthesis was done in water-based medium. For experiments with exciton-plasmon interaction, the same medium was necessary. Different characterization techniques were used to analyze every synthesis.

Experiments for exciton-plasmon interaction were also analyzed using UV-Vis, PL and TCSPC. In PL and TCSPC study, fluorescence quenching was observed with increase in amount of gold solution in CdTe QDs solution indicating interaction between gold (nanospheres and nanorods) and CdTe QDs. Since CdTe QDs shows light-harvesting capabilities and shows high emission yield, the plasmon-exciton interaction may lead to enhancement in electromagnetic field which can have applications in photovoltaic devices.[9],[16]

References

[1] S. K. Kulkarni, *Nanotechnology: Principles and Practices*, Springer International Publishing, **2016**.

[2] N. W. Ashcroft, N. D. Mermin, *Solid State Physics*, Holt, Rinehart And Winston, **1976**.

[3] S. Link, M. A. El-Sayed, *Int. Rev. Phys. Chem.* **2000**, *19*, 409.

[4] G. H. Wannier, *Phys. Rev.* **1937**, *52*, 191.

[5] D. R. Tobergte, S. Curtis, *J. Chem. Inf. Model.* **2013**, *53*, 1689.

[6] P. Capper, I. (Information service), *Properties of Narrow Gap Cadmium-Based Compounds*, INSPEC, The Institution Of Electrical Engineers, **1994**.

[7] L. I. Berger, *Semiconductor Materials*, Taylor & Francis, **1996**.

[8] R. J. Walters, R. V. A. Van Loon, I. Brunets, J. Schmitz, A. Polman, *IEEE Int. Conf. Gr. IV Photonics GFP* **2009**, *9*, 74.

[9] M. Achermann, *J. Phys. Chem. Lett.* **2010**, *1*, 2837.

[10] B. Nikoobakht, M. A. El-sayed, *Chem. Mater.* **2003**, 1957.

[11] J. Turkevich, P. C. Stevenson, J. Hillier, *Discuss. Faraday Soc.* **1951**, *11*, 55.

[12] J. Comenge, V. Puntes, **2011**, 11098.

[13] Y. Chen, Z. Chen, Y. He, H. Lin, P. Sheng, C. Liu, S. Luo, Q. Cai, *Nanotechnology* **2010**, *21*, 125502.

[14] H. Bao, E. Wang, S. Dong, *Small* **2006**, *2*, 476.

[15] N. R. Jana, L. Gearheart, C. J. Murphy, *Langmuir* **2001**, *17*, 6782.

[16] N. N. Lal, B. F. Soares, J. K. Sinha, F. Huang, S. Mahajan, P. N. Bartlett, N. C. Greenham, J. J. Baumberg, *Opt Express* **2011**, *19*, 11256.